PERGAMON

Journal of South American Earth Sciences 16 (2003) 243–257

Journal of
South American
Earth Sciences

www.elsevier.com/locate/jsames

The Choiyoi Group from central Argentina: a subalkaline transitional to alkaline association in the craton adjacent to the active margin of the Gondwana continent

Eduardo J. Llambías[a,*], Sonia Quenardelle[b], Teresita Montenegro[b]

[a]Universidad Nacional de La Plata-CONICET, Calle 1 # 644, 1900 La Plata, Argentina
[b]Departamento de Geología, Facultad de Ciencias Exactas y Naturales, Universidad de Buenos Aires-CONICET, Ciudad Universitaria Pabellón 2, 1428 Buenos Aires, Argentina

Received 31 January 2003; accepted 31 March 2003

Abstract

Permian and Lower Triassic igneous rocks from La Pampa province, central Argentina, are part of the Choiyoi Group, whose extension in Argentina exceeds 500,000 km^2. In La Pampa, the distribution of these outcrops occurs along a NW–SE belt that cuts obliquely across the N–S structures of the Lower Paleozoic rocks. The basement of the Choiyoi Group in western La Pampa consists of Mesoproterozoic to Lower Paleozoic rocks that form part of the exotic Cuyania terrane. In central La Pampa, the basement consists of Lower Paleozoic igneous and metamorphic rocks affected by the Lower Paleozoic Famatinian orogeny.

The Choiyoi Group from La Pampa shares features with the Choiyoi Group elsewhere, such as an abundance of mesosilicic to silicic ignimbrites, subvolcanic domes, and granite plutons emplaced at sallow levels. In La Pampa, we recognize two suites: shoshonitic and trachydacitic to rhyolitic. The shoshonite suite is overlain by trachydacites and rhyolites. The plutonic rocks that belong to the cupola of the intrusive bodies are monzogranitic.

The most significant difference between the Choiyoi Group from La Pampa and that from the Cordillera Frontal and the San Rafael block is that the San Rafael orogenic phase (Lower Permian) is not obvious in La Pampa. Therefore, we cannot attribute to the Choiyoi Group a postorogenic character, as in the Cordillera Frontal or the San Rafael Block. This difference in the tectonic setting is reflected in the composition of the igneous rocks of La Pampa, in that they generally have a higher alkali content with respect to silica, a weak enrichment in TiO_2, and a depletion in CaO. Both suites are transitional from subalkaline to alkaline series.

The shoshonitic suite is rich in clinopyroxene and apatite. Whole-rock compositions have high content of P_2O_5 (0.5–3.9%) and Sr (1320–1890 ppm). Zr is weakly enriched (273–502 ppm), and Nb (29–37 ppm) is depleted. The Th (16–45 ppm) and U (3–14 ppm) content is high.

We postulate a crustal origin for the magma with a source with a calc-alkaline signature. The extensional regime that prevailed during the evolution of the Choiyoi Group favors melting processes.

Keywords: Palabras Claves; Argentina Central; Choiyoi; Magmatismo intraplaca; Permo-Triásico

Resumen

Las rocas ígneas pérmicas y triásico inferior de la provincia de La Pampa, centro de Argentina, forman parte del Grupo Choiyoi, cuya extensión en Argentina excede los 500,000 km^2. En La Pampa sus afloramientos se distribuyen en una faja NO–SE, que corta oblicuamente las estructuras N–S del Paleozoico Inferior. En el oeste de La Pampa el basamento del Grupo Choiyoi está constituido por rocas con edades Mesoproterozoicas a Paleozoico Inferior que pertenecen al terreno de Cuyania. En la parte central de La Pampa el basamento está compuesto por rocas ígneas y metamórficas del Paleozoico Inferior que se correlacionan con las de la fase orogénica Famatiniana.

El Grupo Choiyoi de La Pampa comparte algunas características comunes al Grupo Choiyoi, tales como la abundancia de rocas mesosilícicas a silicica y el desarrollo de plutones graníticos emplazados muy cerca de la superficie. En La Pampa hemos reconocido dos suites: (1) shoshonítica y (2) traquidacítica a riolítica. La suite shoshonítica subyace a las traquidacitas y riolitas. Los plutones son monzograníticos y solamente están expuestos sus cúpulas.

* Corresponding author.
E-mail address: llambias@cig.museo.unlp.edu.ar (E.J. Llambías).

0895-9811/03/$ - see front matter © 2003 Elsevier Ltd. All rights reserved.
doi:10.1016/S0895-9811(03)00070-1

La diferencia más significativa del Grupo Choiyoi de La Pampa con respecto al de la Cordillera Frontal y del Bloque de San San Rafael es que en La Pampa la fase orogénica San Rafael (Pérmico inferior) no es evidente. Por este motivo no se puede atribuir al Grupo Choiyoi de la Pampa un carácter post-orogénico como en las provincias geológicas mencionadas. Esta diferencia en el ambiente tectónico es acompañada en las rocas de La Pampa por un mayor contenido en álcalis respecto a sílice, un débil enriquecicmiento en TiO_2 y empobrecimiento en CaO. Ambas suites son transicionales entre las series sub-alcalinas y alcalinas.

La suite shoshonítica es rica en clinopiroxeno y apatita. Tiene alto contenido de P_2O_5 (0,5 a 3,9%) y de Sr (1320 a 1890 ppm). El Zr está débilmente enriquecido (273 a 502 ppm) y el Nb está ligeramente deprimido (29 a 37 ppm). Los contenidos de Th (16–45 ppm) y U (3–14 ppm) son altos.

Postulamos un orígen cortical para el magma con una fuente con características calco-alcalinas. El regimen extensional que prevaleció durante la evolución del grupo Choiyoi favoreció los procesos de fusión.

Keywords: Palabras Claves; Argentina Central; Choiyoi; Magmatismo intraplaca; Permo-Triásico

1. Introduction

Permian to Lower Triassic mesosilicic and silicic igneous complexes north of 39°S cover an area of at least 200,000 km^2 in central western Argentina and central Chile. This area may be up to 500,000 km^2 according to information from oil exploration boreholes. In Argentina, the volcanic rocks have been included within the Choiyoi Group, which consists of a lower, andesitic to dacitic section and an upper section mainly rhyolitic in composition (Llambías et al., 1993). The volcanic rocks are associated with coeval plutons and form volcano–plutonic complexes (Llambías et al., 1990; Sato and Llambías, 1993), which have been considered the main components of the Choiyoi igneous province by Kay et al. (1989).

The Choiyoi Group is exposed in several geologic provinces, including the Cordillera Frontal, the San Rafael block, and the Cordillera Principal of southern Mendoza and northern Neuquén. In the Sierras Pampeanas, the Choiyoi volcanics occur in two sites. In the La Pampa province, the outcrops extend along a NW–SE belt from southeastern Mendoza to the Buenos Aires province. The easternmost outcrops include the amphibole granites exposed at López Lecube (Fig. 1).

The Choiyoi Group in the Cordillera Frontal and the San Rafael block uncomformably overlies Upper Carboniferous–Lower Permian sedimentary rocks. The San Rafael orogenic phase strongly deformed these rocks during the Lower Permian (Caminos and Azcuy, 1991; Llambías and Sato, 1990, 1995). In La Pampa province, the Choiyoi Group overlies the Permian Carapacha Formation, which is slightly deformed by the San Rafael deformation (Melchor, 1999; Tomezzoli et al., 1999). In the Cordillera Frontal, the Choiyoi Group has a clear postorogenic character (Llambías and Sato, 1995), but in La Pampa, the postorogenic character is not as obvious because of the weak deformation of the Carapacha Formation.

Most geological and geochemical studies of the Choiyoi Group have been carried out in the Cordillera Frontal and San Rafael block, which formed part of the active continental margin of Gondwana during the Late Paleozoic (Caminos, 1979; Nasi et al., 1985; Llambías and Sato, 1990, 1995; Rapalini and Vilas, 1991; Mpodozis and Kay, 1992). Knowledge of the Group in cratonic areas, however, is scarce (Llambías and Leveratto, 1975; Sruoga and Llambías, 1992; Quenardelle and Llambías, 1997). The purpose of this paper is to describe the lithological and geochemical features of the Choiyoi Group in a tectonically stable environment adjacent to the active continental margin.

2. Geological setting

Outcrops of the Choiyoi Group in La Pampa province extend along a NW–SE belt that obliquely cuts the N–S

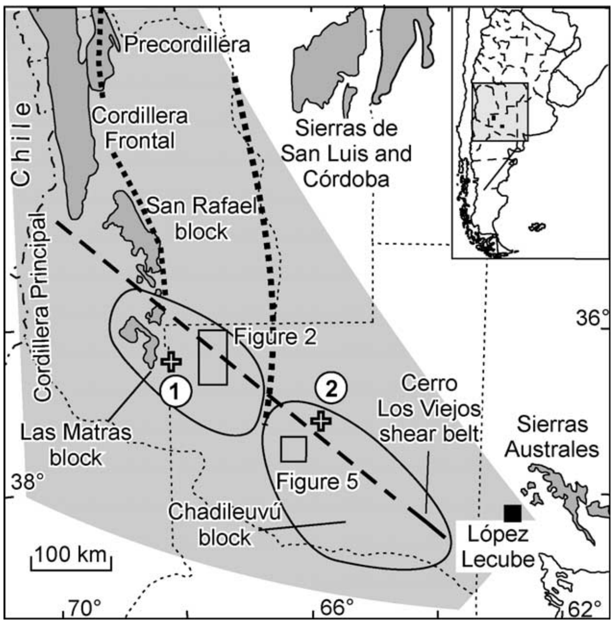

Fig. 1. Location map of the study areas, indicating the Las Matras and Chadileuvú blocks and the assumed continuation of the Cerro de los Viejos shear belt, as well as the location of the Chos Malal granite (1) and the Chacharramendi granite (2). The dotted line indicates the assumed suture between Cuyania and Pampia (Ramos et al., 1998), which correspond to the Las Matras and Chadileuvú blocks, respectively. The broken lines indicate the orogenic front of the Lower Permian San Rafael orogenic phase.

structures of the Middle Proterozoic and Lower Paleozoic units. These units have been grouped into two blocks: Las Matras and Chadileuvú.

The Las Matras block is composed of 1.2 Ga tonalites and trondhjemites, Ordovician limestones (San Jorge Formation), and quartz sandstones of Upper Carboniferous age (Agua Escondida Formation). The tonalites and trondhjemites have been correlated with rocks of similar age in the San Rafael block and the Sierras de Pié de Palo and Umango in the western Sierras Pampeanas (Sato et al., 1999, 2000). The Ordovician limestones are comparable to the limestones of the Ponón Trehue Formation in the San Rafael block and the Precordillera (Melchor et al., 1999). These comparisons enable us to include the basement of the Las Matras block in the Cuyania terrane (Ramos, 1999), which detached from Laurentia and collided with Gondwana during the Ordovician (Dalla Salda et al., 1992; Astini et al., 1995; Vujovich and Kay, 1998; Ramos et al., 1998). The Choiyoi Group rocks intrude and cover all these units.

The Chadileuvú block has a basement of Ordovician metamorphic rocks and Lower Paleozoic granodiorites and monzogranites, correlated with the N–S-trending Famatinian (Lower Paleozoic) orogenic belt of the Sierras de San Luis (Linares et al., 1980; Llambías et al., 1996; Sato et al., 1996; Tickyj, 1999; Tickyj et al., 1999; Sato et al., 2000). Permian sedimentary rocks (Carapacha Formation) overlie these rocks (Melchor, 1999) and were in turn intruded and capped by the rocks of the Choiyoi Group.

3. Geology and petrography of the study areas

To study the Permian–Triassic igneous rocks, we selected two areas (Fig. 1): the Algarrobo del Aguila-Cerro Colón, with an extension of 4500 km^2, located in the Las Matras block, and the La Reforma area of 1200 km^2, located in the western part of the Chadiluvú block. In addition, we studied two small, isolated granite outcrops—the Chos Malal granite in the Las Matras block near the border of the Mendoza province and the Chacharramendi granite in the Chadileuvú block (Fig. 1)—whose geological relationships are uncertain because of the modern sedimentary cover.

In two localities, the igneous bodies are apparently related to volcanic centers. One is located north of Algarrobo del Aguila, where ignimbrites and rhyolite domes surround the granites. These units are a volcano–plutonic complex, which we call the Algarrobo del Aguila igneous complex. The second locality is in La Reforma, where a close relationship is observed among the rhyolite domes, ignimbrites, and highly explosive pyroclastic deposits. We denote this area the La Reforma igneous complex.

3.1. Algarrobo del Aguila–Cerro Colón

3.1.1. Algarrobo del Aguila igneous complex

North of Algarrobo del Aguila, there are several small, isolated outcrops of granites, rhyolite domes, and trachydacite ignimbrites scattered in a 670 km^2 area. The outcrops are discontinuous, but they seem connected in the map of the total magnetic field reduced to the pole, at a scale of 1:250,000 (SEGEMAR, 1998). The distribution of the total intensities of the magnetic field is a semicircle. The granites, coinciding with the lowest intensity of the magnetic field, are in the center, whereas the ignimbrites and domes surround them and have distributions similar to the maximum intensity of the magnetic field. The granites indicate the position of the main igneous conduct and probably correspond to the volcanic center. The domes might follow annular fractures.

3.1.1.1. Granites. The granites are exposed in a 70 km^2 area (Fig. 2). They have a wide variety of textures, including porphyritic, fine-grained equigranular, and aplitic. Miarolas of a few centimeters in diameter, filled with quartz and minor alkaline feldspar, are common.

The most abundant rocks are fine-grained porphyritic monzogranites with fine-grained to aplitic groundmass (Cerro Colorado, Puesto Los Cerros). Quartz phenocrysts are euhedral to subhedral with incipient embayments. The K-feldspar phenocrysts are grayish pink, euhedral, and perthitic and reach 2 cm in length. Biotite is scarce, but zircon, allanite, apatite, fluorite, and opaque minerals are common accessory minerals.

The granite outcrops are interpreted as the cupola of a pluton. The abundance of late aplitic-pegmatitic segregations indicates synmagmatic fractures and moderate water concentrations. The wide variation in the textures and abrupt changes in crystal sizes suggest rapid crystallization from several cooling centers.

Radiometric ages from two K–Ar whole rocks (Linares et al., 1980) yield 256 ± 10 and 236 ± 10 Ma. Two new whole-rock K–Ar ages (Table 1) of the monzogranite porphyry from Cerro Colorado yield 257 ± 5.5 and 198 ± 3.9 Ma.

3.1.1.2. Trachydacites. The trachydacites occur in a sequence of ignimbrites with minor ash and lapilli deposits. Most exposures are in Lomas Altas and Loma Negra. The megascopic aspects are similar to those of andesites and are often described as such (Linares et al., 1980).

The ignimbrites are grayish green to dark gray. They are intensely welded with a moderate crystal content (10–20% according to visual estimates), scarce lithoclasts, laminar fiammes, and a dense devitrified matrix. Crystals are tabular-zoned plagioclase and subhedral to euhedral amphiboles (with rims rich in iron oxide minerals and apatite) altered to an acicular amphibole and scarce biotite. Microphenocrystic apatite is the most abundant accessory.

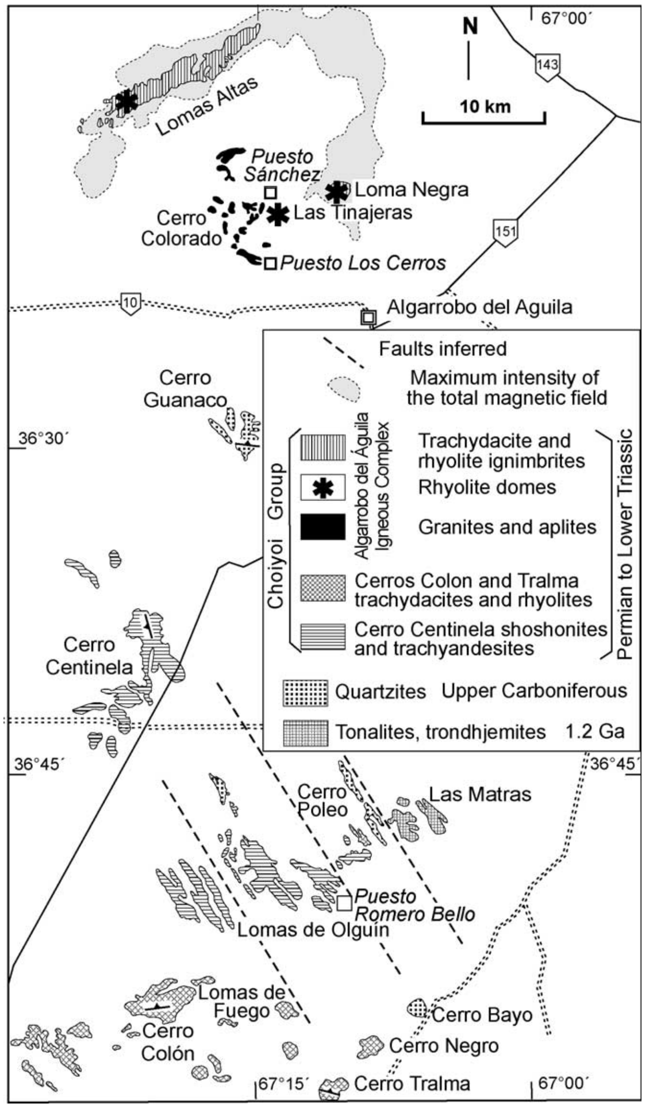

Fig. 2. Geologic map of pre-Triassic outcrops in the area of Algarrobo del Aguila. The maximum intensities of the whole magnetic field are shown shaded, after the Servicio Geológico Minero Argentino map of the total magnetic field reduced to pole, Santa Isabel quadrangle (SEGEMAR, 1998).

The scarce alteration of the rocks consists of secondary quartz, chlorite, epidote, and iron oxides.

The eastern side of Lomas Altas is dominated by thin laminated beds of dense, crystal-rich ash and lapilli deposits rich in plagioclase and K-feldspar and poor in quartz and biotite. According to the total alkali/silica (TAS) diagram (Fig. 7a), they have a dacitic composition close to the trachydacite field. These deposits alternate with thin beds of matrix-supported conglomerates, rich in clasts and similar to the ignimbrites. No clasts of different compositions have been observed.

3.1.1.3. Rhyolite domes. The rhyolite domes intrude the trachydacite ignimbrites at Lomas Altas and Loma Negra and represent the latest event of the volcanic evolution of the Algarrobo del Aguila complex. The rocks have a pale pink color and porphyritic texture, with phenocrysts of plagioclase, K-feldspar, scarce biotite, and quartz. The groundmass is felsitic and compact with intense flow banding a few millimeters thick.

The wide variation in the textures of the igneous bodies—from plutonic to extrusive—suggests that the outcrops of the Algarrobo del Aguila igneous complex are the remnants of an important volcanic center. On the basis of the extension of the outcrops, we can estimate that the volcano would have had a diameter of approximately 30 km. The granites may be the remains of a shallow magmatic reservoir, and the ignimbrites and domes that surround them may have formed part of the volcanic cone. The fine-laminated pyroclastic deposits indicate sporadic phreatomagmatic activity.

3.1.2. Shoshonites and trachyandesites from Cerro Centinela and Lomas de Olguín

The Cerro Centinela and Lomas de Olguín are small hills of less than 150 m. They consist of shoshonite and trachyandesite rheomorphic ignimbrites, lava flows, and lava domes that have been previously described as andesites and included in the El Centinela Formation (Linares et al., 1980). A K–Ar whole-rock age from a Cerro Centinela sample yields 256 ± 10 Ma (Linares et al., 1980).

These rocks are chemically classified as trachytes and trachyandesites (Fig. 7a); according to the potassium content, they are shoshonites (Le Maitre et al., 2002, p. 35). In the K_2O–SiO_2 diagram of Peccerillo and Taylor (1976), they plot in the shoshonite field (Fig. 7b).

Cerro Centinela consists of a sequence of pyroclastic lava flows, striking N10°W and dipping 14°W. At least six major extrusive layers have been recognized with thicknesses ranging from 5 to 15 m, though total thickness reaches 100 m. The ignimbrites are densely welded with flow banding similar to that of lava flows. The rocks are green to grayish pink. The crystal content in the ignimbrites and lavas is moderate, ranging from 15 to 30%. They are composed of tabular-zoned plagioclase (3 mm), prismatic clinopyroxene, and apatite (3 mm). Amphibole is scarce,

Table 1
K–Ar analytical results from the Algarrobo del Águila igneous complex

# Lab	# Field	Rock	Material	K (%)	Error K (%)	^{40}Ar Rad 10^6(ccSTP/g)	^{40}Ar (atm%)	Age (Ma)
7717	Cocol-2	Aplite	WR	3.7874	0.6248	40.60	4.92	256.8 ± 5.5
7718	LCM-7	Aplite	WR	3.9910	0.5000	32.43	2.52	197.9 ± 3.9

has iron oxide rims, and is altered to tremolite–actinolite. Opaque minerals and fluorite are the most abundant accessories. The matrix of the lava flows consists of oriented, needle-like plagioclase and minor clinopyroxene immersed in cryptocrystalline mesostasis. In the ignimbrites, the vitroclasts are strongly deformed, and the fiammes are laminar. The abundance of lithic fragments is variable, ranging from 5 to 15%, and grades up at the base of each flow to lag breccias.

In Lomas de Olguín, a subvolcanic dome has been recognized (36°48′S, 66°06′W) with a porphyritic texture of 35–45% phenocrysts of plagioclase, clinopyroxene, and scarce amphibole. Short tabular microphenocrysts of apatite are abundant and rich in submicroscopic inclusions. Trachyandesites crop out at the southern tip of Lomas de Olguín. They can be distinguished from the shoshonites by amphibole-rich and clinopyroxene-poor mineralogy. Approximately 500 m north of Puesto Romero Bello (36°50′S, 67°15′W), shoshonites and trachyandesites are overlain by trachydacite and rhyolite ignimbrites. This relationship suggests that the shoshonites are older than the trachydacites and rhyolites.

3.1.3. Rhyolites and trachydacites from Cerros Colón and Tralma

Cerro Colón is composed of a succession of rhyolite ignimbrites with thin intercalations of finely laminated pyroclastic deposits. The thickness of the succession is >150 m; neither the top nor the base is exposed. The strike of the beds is N80°E dipping 14° to the NW. Two samples from Cerro Colón were dated (K–Ar, whole-rock) by Linares et al. (1980) at 266 ± 20 and 237 ± 15 Ma. A generalized succession of Cerro Colón is given in Fig. 3. It is schematic because the contacts between the single pyroclastic flows are not easily recognized due to the textural and compositional homogeneity of the flows. The ignimbrites have moderate crystal content (5–20%) locally rich in lithics. Quartz and sanidine are the most common minerals. Plagioclase is less abundant, and biotite is scarce (Fig. 4c and d). Thin laminar lapillitic deposits (Fig. 4a and b) are intercalated between the pyroclastic flows and may be attributed to phreatomagmatic eruptive facies. At the base of the succession are dark trachydacite ignimbrites with a low crystal content ($<10\%$) composed of quartz, plagioclase, and sanidine.

Cerro Tralma (36°59′S, 67°10′W) is a sequence of rhyolite ignimbrites with intercalations of thin laminated pyroclastic deposits. The ignimbrites are intensely welded with rheomorphic textures. The lithoclasts are mainly rhyolitic and minor andesitic in composition, similar in aspect to the trachyandesites of the Lomas de Olguín and Cerro Negro.

3.2. La Reforma

La Reforma (Fig. 5) is close to the union of the Chadileuvú and Las Matras blocks. In this area, outcrops

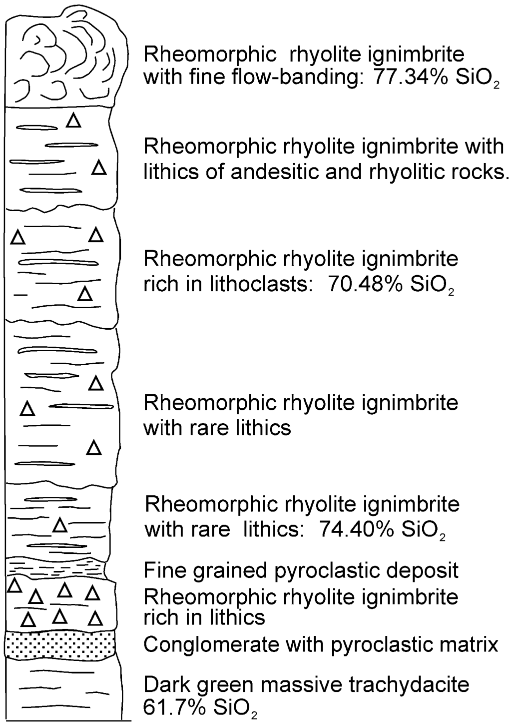

Fig. 3. Schematic columnar section, not to scale, of the volcanic sequence of Cerro Colón, indicating the SiO_2 content of the analyzed rocks.

are small and scattered. The oldest rocks are sedimentary rocks of the Perrmian Carapacha Formation, whose maximum thickness is 630 m (Melchor, 1999). The Choiyoi igneous rocks intrude and overlie the Carapacha Formation.

The La Reforma volcanic complex consists of rhyolite domes, finely laminated pyroclastic deposits, rheomorphic ignimbrites, and scarce rhyolite dikes intruding the Carapacha Formation (Fig. 5). The domes are exposed at Cerro El Divisadero and Cerro Choique Mahuida. The rocks are pinkish gray, with porphyiritic textures and aphanitic-microgranular groundmass. The phenocrysts are euhedral sanidine with microscopic inclusions of plagioclase, euhedral to subhedral quartz, and biotite altered to chlorite. Euhedral amphibole has been entirely altered to tremolite-actinolite, epidote, chlorite, and opaque minerals. Microphenocrysts of apatite have prismatic sections and are oriented.

The trachydacite ignimbrites are crystal rich, intensely welded, and entirely devitrified. They are dark gray to dark green and rich in lithics. Zoned, prismatic plagioclase ($An_{35\text{-}30}$) is the most abundant mineral and is altered to sericite, calcite, epidote, and argillaceous minerals. The amphibole is entirely altered to chlorite and iron oxide minerals, whereas the biotite is intensely altered to chlorite and iron oxide minerals. The rhyolite ignimbrites are pink gray and contain plagioclase, K-feldspar, and quartz. Biotite is rather scarce.

Cerro La Ramadita (37°29′S, 66°28′W) consists of pyroclastic deposits that contain blocks of exotic limestones partially transformed into skarn. The beds have light grayish

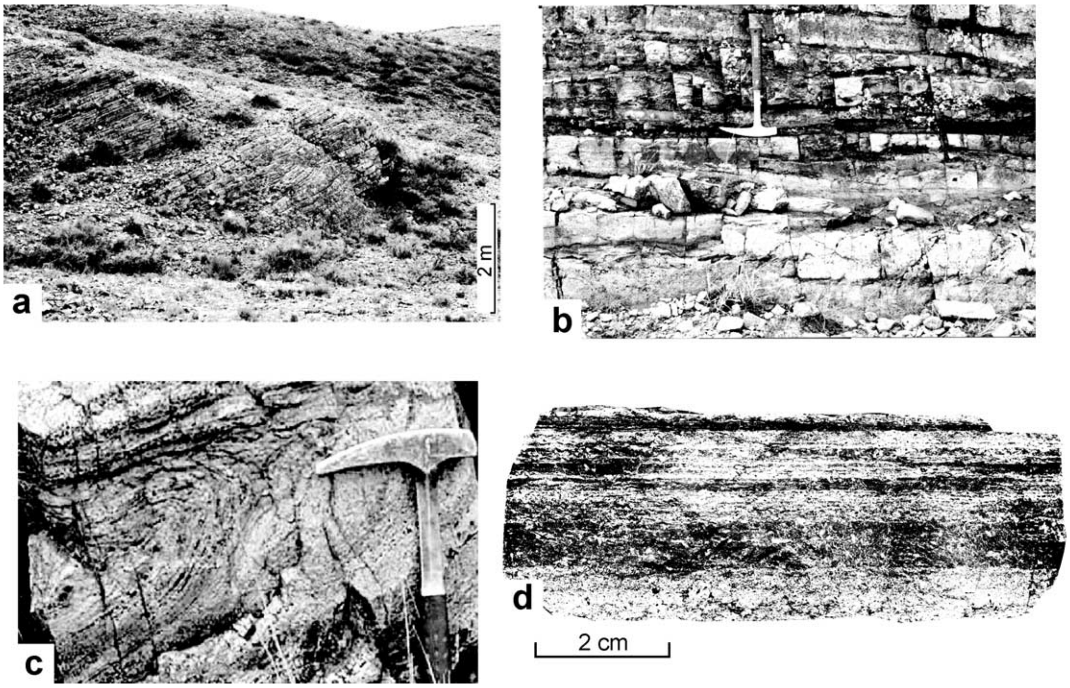

Fig. 4. Photographs of rhyolite pyroclastic deposits from Cerro Colón (a, b, c) and Tralma (d). (a) Laminated pyroclastic beds intercalated between the ignimbrites. (b) Detail of (a) to show the internal structures of the layers that wedge laterally in short distances and thicken in low areas. The head of the hammer indicates the bottom of the beds. These structures are typical of surge deposits. (c) and (d) Rheomorphic ignimbrites. (c) The rheomorphic flow is evidenced by the folded flow layers; (d) the flow layers are planar and consist of dark glassy layers and less compact glassy gray layers.

colors and are up to 2 m thick. The most abundant components are tabular K-feldspar, plagioclase, quartz, ferromagnesic minerals altered to epidote, opaque minerals, and chlorite. Devitrified vitroclasts are in proportion of 2–5%. Microgranular calcite cements the components. The beds are finely laminated (millimeters to centimeters) and show evidence of intrastratal deformation and internal erosive surfaces (Fig. 6). The limestone blocks are up to 1 m in diameter and have a grayish to light blue color. They consist of recrystallized calcite, garnet, and subordinate quartz.

The limestone blocks included into the pyroclastic rocks indicate a calcareous basement in the volcanic roots and highly explosive volcanic facies. The aspect of the blocks is

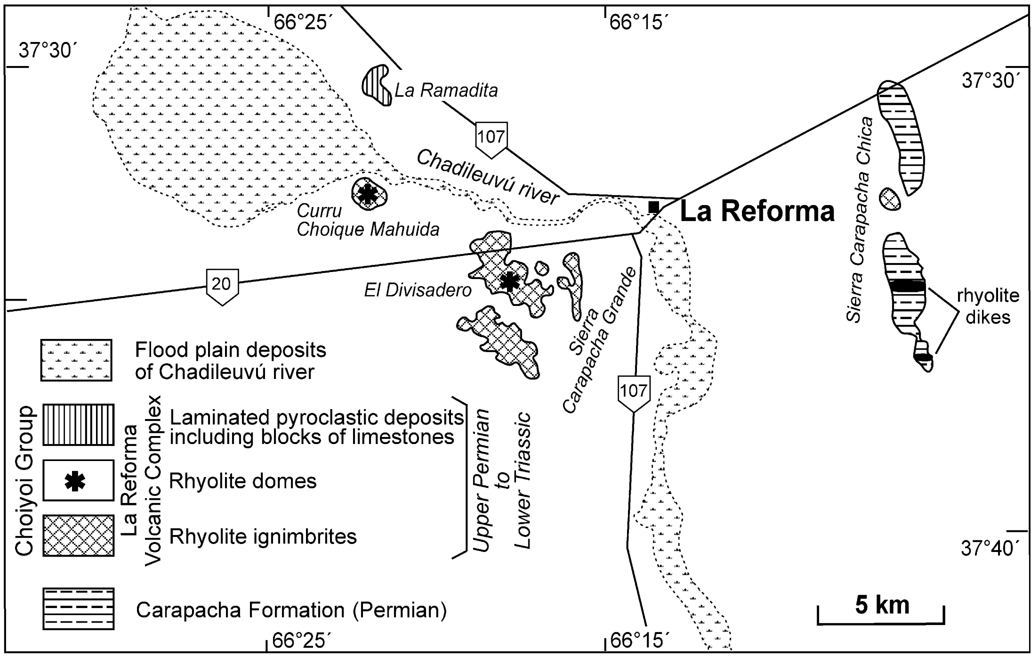

Fig. 5. Geological map of the Permo-Triassic igneous rocks of La Reforma, La Pampa.

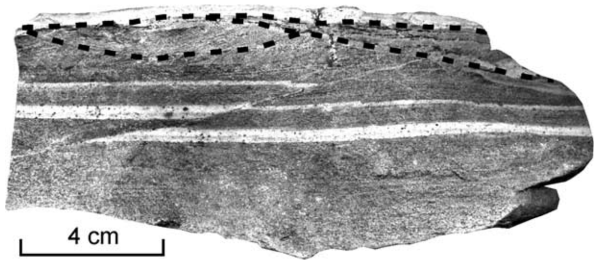

Fig. 6. Detail of the laminar pyroclastic deposits of Cerro La Ramadita, La Reforma, which are characterized by contemporaneous perturbations during deposition. From lower left to upper right, there is an intrastratal fracture truncated by the top layers. Cross-bedding structures are common, as shown at the top.

similar to that of the limestones of the San Jorge Formation (Ordovician) that crop out 40 km to the northwest.

3.3. Isolated granites

3.3.1. Chacharramendi granite

The Chacharramendi granite (37°18′S, 65°46′W), 10 km west of Chacharramendi, is only exposed in a small quarry. This pink grayish, granular granite is composed of coarse crystals of K-feldspar, euhedral to subhedral quartz, oligoclase, and scarce biotite. Apatite, zircon, and opaque minerals are accessory, and synmagmatic aplite veins are common. A K–Ar, whole-rock dating yields an age of 220 ± 10 Ma (Linares et al., 1980), younger than the other dated rocks from the Choiyoi Group of La Pampa.

3.3.2. Chos Malal granite

Small outcrops of the Chos Malal granite (36°48′S, 68°10′W) occur near the province of Mendoza. They are covered by modern sediments and basaltic lava flows. The granite is pink gray, with a medium to fine granular texture, and consists of subhedral to anhedral quartz, tabular K-feldspar, weakly zoned plagioclase, and scarce biotite altered to chlorite. As accessories, opaque minerals, fluorite, allanite, and zircon appear. The aplite facies is transitional to the granite and forms thin veins with scarce garnet. A K–Ar whole-rock dating yields an age of 250 ± 10 Ma (Linares et al., 1980).

3.3.3. Chemical characteristics

Representative samples of the units were analyzed. Caution is necessary with granite samples because they come from the volatile-enriched cupola of the plutons, and subsolidus reactions could affect the primary magmatic composition. Major oxides were analyzed by fusion-ICP, and trace elements and REE were analyzed by fusion-ICP MS at the Activation Laboratories (Canada). The results are presented in Table 2.

The analyzed volcanic rocks fall in three groups, according to Le Maitre et al. (2002) diagram: rhyolites, trachydacites, and trachytes (Fig. 7a). The trachydacites plot close to the line that divides the fields of trachyandesites, andesites, and dacites. The trachytes are in the alkaline field, according to the subdivision by Irvine and Baragar (1971), but differ from the typical alkaline series in that they have 2.4–5.7% normative hyperstene and.1–4.9% normative quartz and are associated with silicic rocks.

All the samples analyzed are rich in potassium (Fig. 7b), and in Peccerillo and Taylor's (1976) diagram, the trachytes from Cerro Centinela and Lomas de Olguín plot on the field of the shoshonite series. The K_2O/Na_2O ratio ranges from 0.84 to 1.18. Although among the analyzed samples there are no rocks with $SiO_2 < 55\%$, the chemical characteristics agree with the shoshonite association described by Morrison (1980): low TiO_2 ($<1.3\%$) and enrichment in P, Rb, Sr, Ba, and Pb. The trachyandesites from southern Lomas de Olguín plot in the field of the high-K series, but any conclusion about these samples is preliminary because the volatile content is high (2.38 and 3.12%), which suggests alteration. The K_2O/Na_2O ratio in the rhyolites ranges from 1.15 to 1.59; in the monzogranites from Chos Malal and Algarrobo del Aguila, it ranges from 1.06 to 1.48.

The magnesium number ($Mg\# = Mg/Mg + Fe^{+2}, Fe^{+2}$; calculated after Le Maitre's (1976) index) for the shoshonites and trachydacites is similar, ranging from 39 to 45 and from 37 to 44, respectively. The CaO content (Fig. 8) is smaller than the best fit of the Arequipa segment of the Coastal batholith of Perú (Pitcher et al., 1985, pp. 291–292). We compared our samples with the Arequipa segment because it represents a typical calc-alkaline magmatic arc emplaced on an igneous and metamorphic basement.

The TiO_2 correlates negatively with SiO_2, and samples with $SiO_2 < 66\%$ are enriched with respect to the best fit of the Arequipa segment of the Coastal batholith from Perú (Fig. 8). The P_2O_5 correlates negatively with SiO_2 (Fig. 8), and the slope of samples with $SiO_2 < 66\%$ is steeper than that for the rhyolites. The content of P_2O_5 in the shoshonites is unusually high, in agreement with an abundance of apatite, and reaches 3.8% (CC99-1), though more frequent values are close to 0.8%. These contents are several times higher than those of the calc-alkaline series, whose average values range from 0.1 to 0.2% P_2O_5 (Gill, 1981, p. 112). In addition, the content of P_2O_5 is higher than the best fit for the Arequipa segment.

The Rb content of the shoshonite rocks from Cerro Centinela and Lomas de Olguín (Table 2) ranges from 101 to 186 ppm, with an average of 149 ppm ($n = 9$). This range agrees with the contents of the shoshonite association (Morrison, 1980) and is enriched with respect to rocks with a similar proportion of SiO_2 in the calc-alkaline series. The abundance of Rb in the trachyandesites, trachydacites, and rhyolites is depleted with respect to the best fit for the Arequipa segment (Fig. 8).

The spider diagrams (Fig. 9) of trace elements and REE have been normalized to primordial mantle and chrondrite, respectively (Taylor and McLennan, 1985). The shoshonites and trachyandesites from Cerro

Table 2
Representative chemical analyses from the Choiyoi Group of northwestern La Pampa, central Argentina

	Algarrobo del Águila Igneous Complex													Rhyolite and Trachydacite Ignimbrites						
	Granites					Domes			Ignimbrites					Cerro Colón				Cerro Tralma		
	LCM 4	LCM 1	LCM 5	LCM 7	CoCol 2	SAN 1	JAR 2	LMN 2	JAR 1	JAR 3	JAR 5	LMAS	LMN 1	Col9822	Col9816	Col9817	Col9819	PU 4	PU 6	PU 7
SiO_2	75.76	78.15	77.72	77.71	76.89	77.82	76.88	77.85	62.81	65.28	60.44	62.04	61.38	61.57	74.46	70.48	77.34	71.87	69.14	66.41
TiO_2	0.14	0.10	0.10	0.11	0.09	0.05	0.08	0.05	0.75	0.63	0.95	0.87	1.00	0.66	0.12	0.41	0.04	0.14	0.27	0.47
Al_2O_3	12.57	12.38	12.32	12.33	12.40	12.33	12.39	11.97	15.22	15.52	15.00	14.64	14.66	17.31	13.49	14.07	12.56	15.04	14.77	15.36
Fe_2O_3	1.58	0.95	1.08	0.95	0.96	0.88	0.87	1.34	5.84	4.51	6.42	6.24	6.05	5.18	2.00	2.72	1.22	2.92	3.26	3.61
MnO	0.04	0.03	0.03	0.04	0.02	0.01	0.03	0.02	0.12	0.08	0.11	0.07	0.09	0.09	0.03	0.06	0.06	0.05	0.06	0.07
MgO	0.23	0.06	0.08	0.11	0.07	0.05	0.06	0.05	3.04	2.11	2.91	2.31	3.39	1.46	0.16	0.74	0.06	0.21	0.61	1.25
CaO	0.64	0.44	0.42	0.47	0.54	0.25	0.64	0.39	4.33	3.96	5.04	3.87	4.85	4.72	0.79	2.02	0.58	1.00	1.69	3.02
Na_2O	3.35	3.47	3.36	3.45	3.57	4.05	3.36	4.03	4.34	3.92	4.32	3.63	3.35	4.06	4.20	2.87	3.75	3.58	3.42	3.60
K_2O	4.68	5.06	4.98	4.77	4.66	4.67	5.33	3.96	2.96	3.57	2.70	2.88	4.22	2.95	4.74	5.12	4.16	4.86	4.29	3.18
P_2O_5	0.03	0.02	0.02	0.02	0.02	0.02	0.01	0.02	0.35	0.32	0.49	0.34	0.47	0.37	0.02	0.06	0.02	0.15	0.15	0.17
LOI	0.61	0.27	0.20	0.13	0.23	0.23	0.14	0.27	0.89	0.74	1.35	3.14	0.70	0.57	0.48	0.61	0.83	0.47	0.87	1.42
Total	99.62	100.94	100.29	100.08	99.44	100.35	99.80	99.94	100.64	100.65	99.72	100.02	100.16	98.96	100.48	99.15	100.62	100.30	98.50	98.55
Trace elements (ppm)																				
Sr	91.1	34.6	27.3	31.4	26.4	8.3	249	207	812	790	1100	748	1310	739	115	247	90	156	226	423
Cs	3.2	6.8	3.7	13	7.1	4.2	0.9	1.4	3.6	5.3	1.4	3.8	3.3	3.8	3.8	6.3	3.2	5.5	5.0	1.5
Rb	206	245	209	241	226	229	106	127	67	68	56	90	91	73	159	155	135	174	146	103
Ba	234	72	63	92	43	18	588	459	1240	1370	1110	1290	1530	1360	1160	1380	712	1970	1680	1030
Th	31.3	40.4	41.6	39.2	42.9	36.5	25.2	31.9	5.05	5.26	4.44	9.18	9.17	7.31	14.8	17.2	10.3	14.7	13.9	10.8
U	3.28	4.7	4.67	4.57	13.9	5.44	6.46	7.38	1.78	1.67	1.68	2.53	2.14	1.78	2.28	4.51	2.76	3.87	3.68	2.61
Ta	2.26	2.87	2.78	3.58	5.35	2.99	2.02	2.05	0.62	0.55	0.65	0.59	0.59	0.52	0.94	0.97	3.1	1.9	2.3	1.5
Nb	20	25	22	22	51	32	22	20	8.6	8.1	9.6	10	8.8	8.2	13	14	9.5	13.3	12.2	9.9
Ce	75	67.6	61.7	66.2	47.4	51.4	46.7	53.2	51.5	64.7	64.9	81.2	92	82	94.3	108	52.4	100	91.5	74.9
Zr	99	101	83	96	91	100	96	87	153	211	161	243	207	222	157	255	93	157	195	222
Hf	3.4	4	3.4	3.6	4.4	4.8	3.8	3.9	3.9	5	4.2	6	5.7	5.3	5	8.1	3.4	4.9	5.4	5.7
Y	19	24	21	28	42	34	19	24	22	16	18	21	18	22	28	35	22	34.1	31.4	23.8
V	12	16	15	37	7	41	28	30	121	73	114	181	134	47	6	32	− 5	11	28	82
Cr	13	11	10	17	12	10	11	20	76	33	44	67	79	12	12	28	74	176	159	88
Co	1.1	0.6	2.6	1.8	− 0.5	− 0.5	0.7	− 0.5	16	9.3	16	11	31	6.8	2	3.5	28	13	19	18
Ni	12	− 10	− 10	15	− 10	− 10	− 10	11	39	29	38	38	57	21	− 10	20	56	113	59	58
Ga	16	18	16	16	18	20	16	15	20	20	21	22	20	20	20	19	15	23	21	21
Tl	0.66	1.48	0.92	0.89	0.46	1.01	0.21	0.28	0.57	0.38	0.17	1.20	0.36	0.19	1.57	0.39	0.65	0.91	0.49	0.36
Pb	13	24	19	23	11	23	23	11	17	15	14	14	19	11	42	21	20	24	10	20
Rare earth elements (ppm)																				
La	38.10	36.00	28.80	30.30	20.00	21.40	21.00	20.30	24.90	32.10	31.90	38.10	44.20	39.70	48.20	52.70	24.39	46.95	42.41	36.79
Ce	75.00	67.60	61.70	66.20	47.40	51.40	46.70	53.20	51.50	64.70	64.90	81.20	92.00	82.00	94.30	108.00	52.40	100.49	91.53	74.88
Pr	6.95	7.07	5.82	6.44	5.11	6.23	4.81	5.71	5.33	6.68	6.91	8.31	9.46	8.23	9.38	10.96	5.77	10.67	9.84	7.72
Nd	24.80	26.60	20.70	22.90	20.40	26.10	17.60	23.30	23.40	26.60	31.40	34.70	39.20	35.00	36.30	44.20	21.52	41.08	36.82	28.78
Sm	4.40	5.10	4.14	4.57	5.55	6.33	3.34	5.42	4.72	4.70	6.15	6.68	7.32	6.26	6.38	8.16	4.41	7.89	6.92	5.28
Eu	0.38	0.24	0.21	0.24	0.18	0.04	0.16	0.16	1.15	1.41	1.61	1.58	1.86	1.52	0.62	1.23	0.40	1.30	1.27	1.27
Gd	3.54	4.08	3.19	0.77	5.03	5.12	2.78	4.28	3.59	3.75	4.46	5.02	5.46	4.71	5.05	6.58	3.70	6.47	5.83	4.26
Tb	0.53	0.68	0.52	0.65	1.10	0.97	0.52	0.72	0.57	0.51	0.68	0.71	0.70	0.69	0.80	1.06	0.63	1.04	0.92	0.68
Dy	2.97	3.55	2.99	3.60	6.26	5.30	2.91	3.64	3.29	2.67	3.42	3.61	3.58	3.84	4.33	5.63	3.61	5.83	4.96	3.79
Ho	0.55	0.66	0.62	0.70	1.28	1.00	0.58	0.69	0.67	0.51	0.60	0.66	0.64	0.70	0.82	1.10	0.74	1.10	0.97	0.75
Er	1.83	2.16	1.95	2.34	3.93	3.16	1.85	2.20	1.98	1.50	1.73	1.89	1.76	2.09	2.57	3.35	2.30	3.28	2.93	2.24
Tm	0.33	0.41	0.36	0.45	0.72	0.57	0.33	0.38	0.31	0.22	0.26	0.27	0.24	0.32	0.44	0.53	0.36	0.50	0.45	0.35
Yb	2.13	2.65	2.47	2.86	4.70	3.52	2.15	2.47	2.06	1.41	1.63	1.73	1.60	2.06	2.69	3.15	2.38	3.13	2.73	2.39
Lu	0.34	0.41	0.40	0.44	0.72	0.53	0.34	0.41	0.32	0.24	0.25	0.25	0.24	0.32	0.40	0.48	0.35	0.46	0.40	0.34

	Shoshonites									Trachyandesites		La Reforma Igneous Complex					Chacha-rramendi Granite	Chos Malal Granite	
	Cerro Centinela						Lomas de Olguín			Lomas de Olguín		Domes		Ignimbrites					
	CEN 2	CEN 3	CEN 4	CEN 6	CC99-1	CC99-2	PU 3	PU 9	PU 14	PU 1	PU 2	LP61	LP63	LP64	LP65	LR1	LP73	CHM3	CHM4
SiO_2	59.30	61.39	60.25	59.45	55.21	57.70	58.16	59.18	59.41	55.65	56.18	72.23	74.53	69.85	69.68	64.78	76.30	77.64	77.60
TiO_2	1.11	0.82	1.00	0.91	1.07	1.04	1.02	0.88	0.88	0.91	0.84	0.22	0.19	0.39	0.32	0.679	0.16	0.04	0.05
Al_2O_3	16.01	16.26	16.00	16.46	16.20	15.70	15.36	15.39	15.71	16.11	16.89	14.75	14.60	14.89	15.11	15.83	12.76	11.82	12.56
Fe_2O_3	6.32	4.89	5.43	5.33	6.28	6.47	7.25	6.30	5.72	7.30	7.47	1.30	1.14	2.08	1.81	4.66	0.99	0.86	1.02
MnO	0.06	0.08	0.08	0.08	0.12	0.08	0.12	0.11	0.09	0.19	0.15	0.02	0.02	0.04	0.03	0.07	0.03	0.01	0.05
MgO	2.26	1.79	2.32	2.33	3.47	1.88	2.34	2.11	2.25	2.34	2.83	0.36	0.18	0.68	0.63	1.40	0.14	0.01	0.03
CaO	3.15	3.11	3.99	3.41	4.06	4.39	4.69	3.84	4.56	6.96	5.68	1.55	0.39	1.83	2.16	2.69	0.63	0.21	0.34
Na_2O	4.58	5.65	5.48	5.22	4.20	5.61	4.74	4.88	4.15	3.85	3.73	3.72	3.18	4.64	4.17	5.28	3.43	3.93	4.28
K_2O	5.41	5.21	4.58	5.69	4.75	3.48	4.96	4.20	4.54	1.98	2.39	4.40	4.19	4.10	4.13	3.26	4.63	4.41	4.55
P_2O_5	0.83	0.54	0.64	0.65	3.87	0.69	0.62	0.59	0.51	0.32	0.37	0.06	0.04	0.13	0.10	0.30	0.02	0.01	0.04
LOI	1.57	0.48	0.78	1.31	0.90	1.58	0.86	1.18	0.47	3.12	2.38	1.11	1.20	1.19	1.35	1.25	0.56	0.03	0.18
Total	100.60	100.24	100.54	100.84	100.12	98.62	100.11	98.67	98.29	98.72	98.91	99.50	99.47	99.43	99.17	100.19	99.49	98.97	100.69
Trace elements (ppm)																			
Sr	1640	1680	1890	1710	1530	1320	1760	1750	1750	753	1130	623	299	899	1125	811	94	6.67	11.3
Cs	5.2	3.5	3.8	6.6	19.5	2.0	4.3	1.6	2.9	4.7	4.3	2.74	3.47	1.6	1.82	2.8	2.92	1.9	3.5
Rb	170	170	138	174	186	101	137	135	126	44	65	128	154	98	87	103	283	169	203
Ba	1570	1540	1510	1500	1320	1360	1720	1510	2080	1400	1360	995	710	1610	1807	1340	257	7.3	42
Th	45.3	36.2	24.3	37.4	30.7	20.0	23.5	17.1	15.8	6.97	8.42	3.93	4.11	6.40	8.05	12.2	33.04	56.3	26.2
U	13.6	9.63	8.64	7.76	4.71	3.74	7.48	3.15	4.36	1.92	2.71	0.87	0.97	1.29	1.34	2.93	1.49	6.58	2.92
Ta	1.88	1.71	1.44	1.91	2.2	1.6	1.6	1.7	1.8	0.9	1.0	1.23	1.64	1.59	1.55	2.2	4.19	7.61	2.23
Nb	37	33	29	37	33.6	22.3	22.4	19.8	12.3	7.3	9.9	5.9	6.8	7.9	6.8	24.4	24.1	65	30
Zr	502	484	399	391	330	375	353	343	273	103	117	96	91	155	147	255	107	197	100
Hf	12	11	9.3	10	8.1	7.9	8.1	7.8	6.8	2.6	3.1	3.14	3.15	4.97	4.7	6.4	4.32	16	5.7
Y	17	12	15	16	17.5	16.0	24.1	19.2	21.7	14.1	16.1	8	6	6	6	22.1	12	125	47
V	124	74	118	92	120	108	133	100	130	158	172	14	21	29	23	109	15	− 5	− 5
Cr	60	36	89	42	681	199	296	294	162	291	243	− 10	17	− 10	− 10	205	18	12	12
Co	13	11	14	16	26	20	22	21	32	26	27	23.9	22.6	29.8	26.7	25	47.9	− 0.5	59
Ni	50	34	58	42	409	126	130	131	100	142	148	− 5	− 5	− 5	− 5	124	11	− 10	47
Ga	27	27	26	29	28	28	27	25	25	27	22	21	21	24	22	22	20	26	21
Tl	0.50	0.52	0.20	0.14	0.10	0.38	0.33	0.05	0.48	0.16	0.54	0.66	0.6	0.44	0.34	0.22	1.53	0.45	1.43
Pb	41	42	19	51	16	22	20	7	18	− 5	9	21	12	24	23	− 5	36	17	33
Rare earth elements (ppm)																			
La	66.50	65.00	64.70	64.30	64.54	60.48	72.47	64.31	68.45	28.82	34.87	18.74	14.01	45.97	44.82	48.3	43.68	12.4	17.2
Ce	101.00	126.00	116.00	104.00	129.78	122.08	144.35	129.14	139.25	52.10	61.86	36.85	28.06	88.95	85.64	95.9	84.89	37.1	45.7
Pr	13.17	12.37	12.70	12.22	13.55	12.96	15.45	13.68	15.06	5.46	6.79	3.52	2.79	8.26	8.19	9.60	7.62	4.762	5.22
Nd	54.80	48.90	52.90	48.60	51.94	50.99	60.87	52.35	59.61	21.77	26.73	14.54	11.82	35.77	33.43	35.7	28.48	20.5	22
Sm	9.19	7.51	8.62	8.12	8.50	8.31	10.86	8.66	9.94	4.08	4.87	2.78	2.22	5.57	4.70	5.92	4.79	7.89	6.44
Eu	2.20	1.80	2.09	1.98	2.54	2.51	3.22	2.62	2.84	1.43	1.80	0.62	0.50	1.29	1.14	1.58	0.63	0.038	0.13
Gd	6.28	5.35	5.84	5.53	6.18	5.79	7.87	6.14	6.92	3.67	4.42	2.16	1.88	3.62	3.50	4.81	4.01	7.59	5.29
Tb	0.75	0.53	0.63	0.63	0.72	0.70	0.99	0.73	0.84	0.52	0.62	0.29	0.24	0.36	0.33	0.70	0.47	2.02	1.2
Dy	3.29	2.37	2.90	3.01	3.34	3.11	4.65	3.58	4.07	2.57	3.12	1.29	1.14	1.17	1.05	3.61	1.99	12.6	7.31
Ho	0.52	0.37	0.45	0.47	0.56	0.51	0.76	0.58	0.71	0.45	0.54	0.25	0.22	0.19	0.17	0.69	0.38	2.77	1.47
Er	1.54	1.11	1.34	1.37	1.46	1.30	1.97	1.57	1.84	1.26	1.59	0.75	0.60	0.49	0.41	1.97	1.10	9.42	4.59
Tm	0.19	0.14	0.16	0.18	0.20	0.17	0.26	0.21	0.25	0.16	0.23	0.10	0.08	0.05	0.05	0.27	0.17	1.894	0.84
Yb	1.26	0.91	1.01	1.17	1.27	1.11	1.61	1.40	1.62	1.03	1.40	0.66	0.56	0.32	0.32	1.77	1.14	13.5	5.59
Lu	0.20	0.15	0.15	0.18	0.19	0.16	0.23	0.21	0.24	0.16	0.21	0.10	0.09	0.05	0.05	0.27	0.19	2.292	0.85

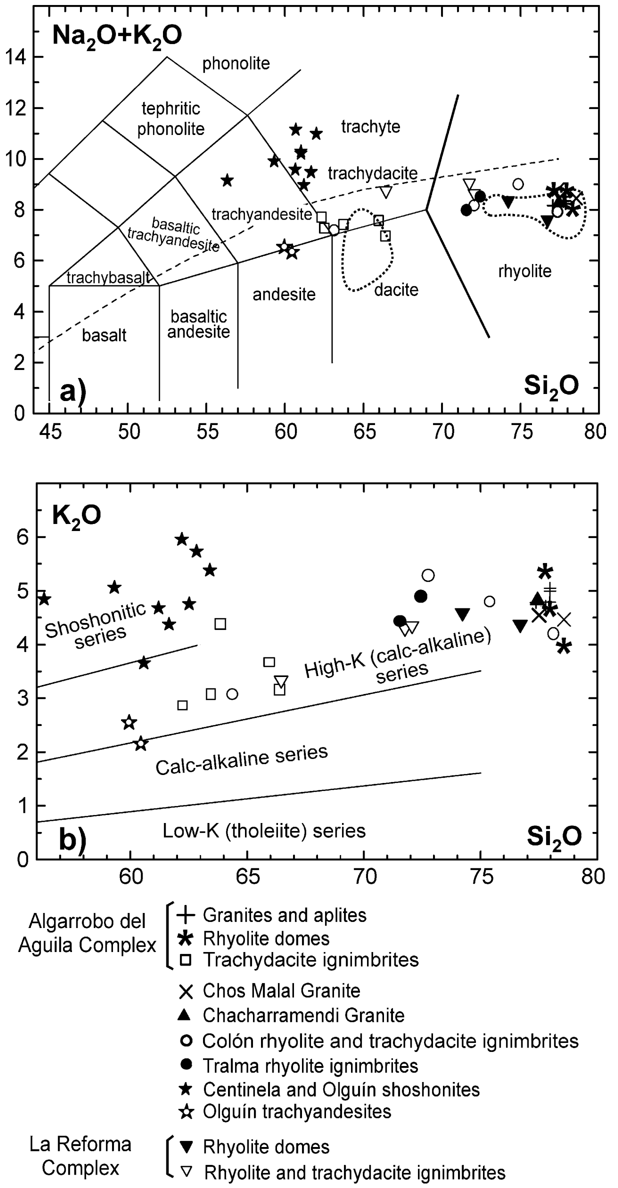

Fig. 7. (a) Total alkalis versus silica (TAS) diagram after Le Maitre et al. (2002). The broken line separates alkaline from sub-alkaline fields, according to Peccerillo and Taylor (1976). The two circular areas delimited by dotted lines show the composition of the volcanic rocks and dikes of the Choiyoi Group from the Colangüil batholith (Llambías and Sato, 1995). (b) K_2O versus SiO_2 diagram, with the subdivisions of the alkaline series after Peccerillo and Taylor (1976). The samples that plot on the trachyte field in the TAS diagram also plot on the field of the shoshonite series.

Centinela and Lomas de Olguín show a relative enrichment in Ba, Th, U, Sr, P, Y, and Zr and a relative depletion in Nb. The REE diagrams (Fig. 10) maintain a small dispersion, as do those for the trace elements. The trachyandesites are less enriched in LREE than are the shoshonites. The $La/Yb_{(n)}$ ratio of shoshonites and trachyandesites ranges from 36 to 48 and is the highest of the analyzed samples, comparable to the ratio of the trachyandesites from Sierra Chica, located 210 km to the SE (Quenardelle and Llambías, 1997).

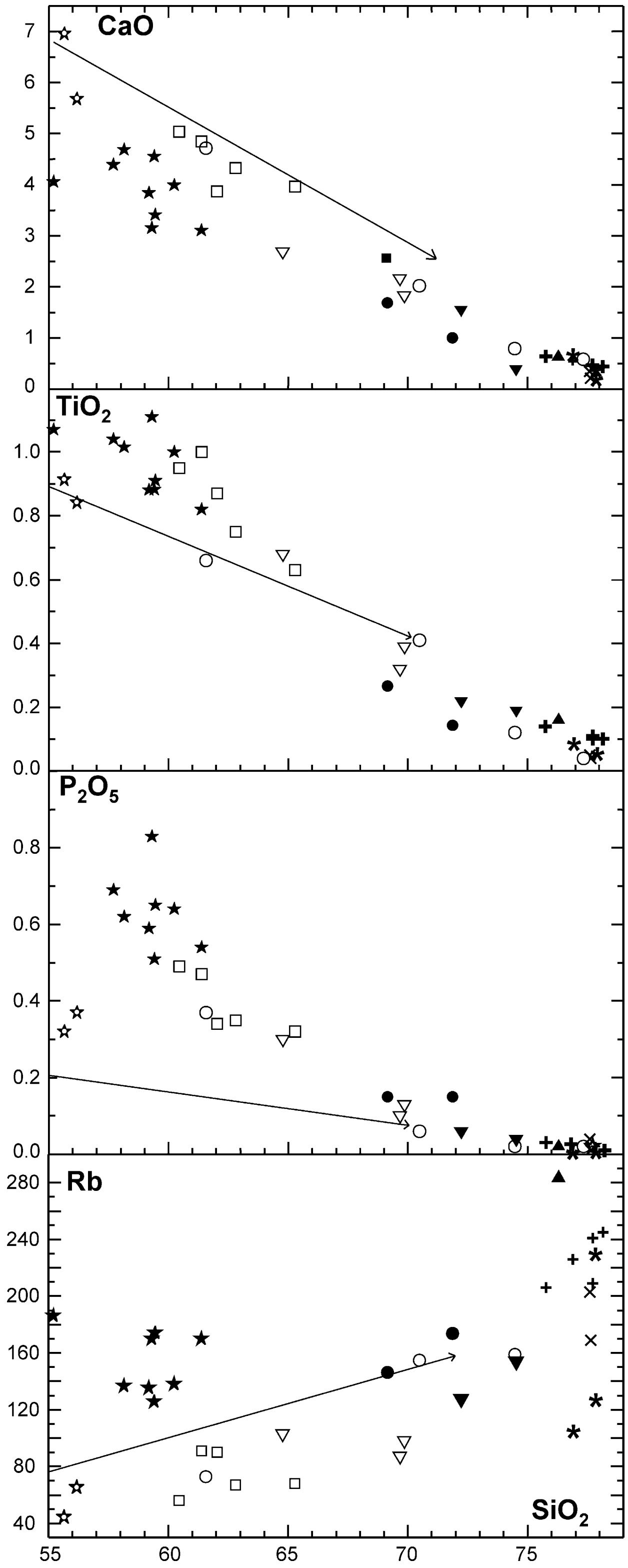

Fig. 8. Harker plots of selected oxides for the Choiyoi Group of La Pampa. The arrows show the best fit for samples from the Arequipa segment of the Coastal batholith of Peru (Pitcher et al., 1985, pp. 191–192), which represents a typical calc-alkaline series emplaced in an igneous, metamorphic basement. Samples from La Pampa are depleted in CaO and enriched in P_2O_5 and TiO_2. Symbols are as in Fig. 7.

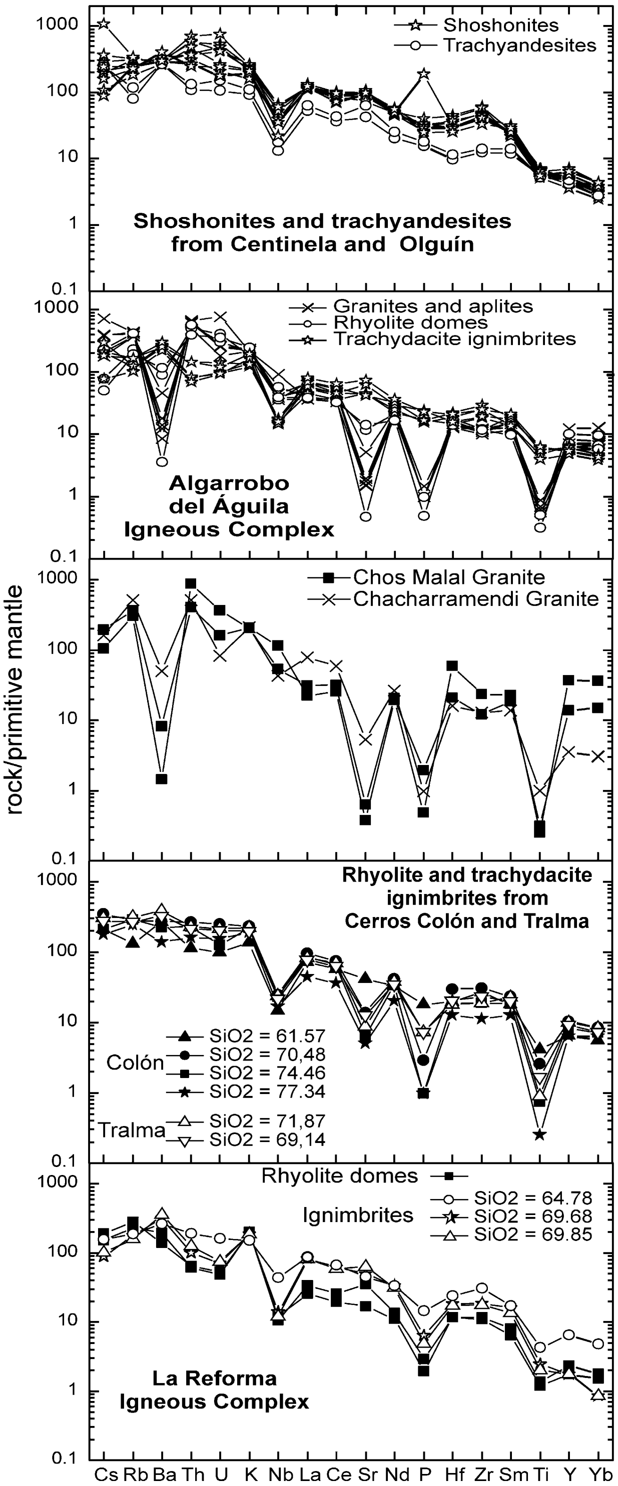

Fig. 9. Spider diagrams normalized to primordial mantle (Taylor and McLennan, 1985). A common feature of all samples is the enrichment of Th and U and weak depletion of Nb and Ti. Shoshonites are also enriched in Sr, P, and Zr.

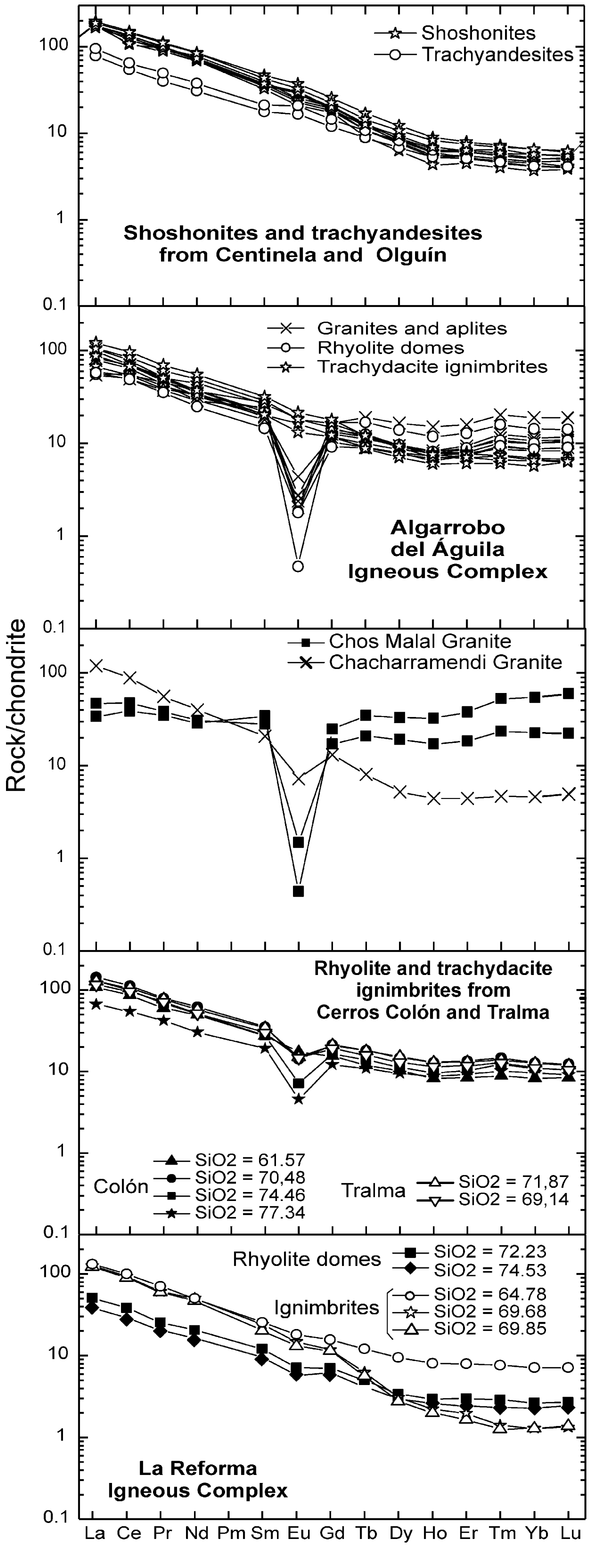

Fig. 10. REE diagrams normalized to chrondrite (Taylor and McLennan, 1985).

The trachydacites from Algarrobo del Aguila and Cerro Colón show a relative enrichment in Ba, Sr, and Zr and a depletion in Nb, Ti, Th, and U. The granites and rhyolites are strongly depleted in Ba, Nb, Sr, P, and Ti. The rhyolite domes are similar, suggesting a close relationship to the granites. The La/$Yb_{(n)}$ ratios decrease from the trachydacites to the rhyolites, and the Eu depletion is characteristic of more silicic rocks.

The trace element abundance in the La Reforma igneous complex is similar to that of the Algarrobo del Aguila complex. The less silicic samples show enrichment in Ba, Th, U, Sr, and Zr and depletion in Nb and Ti. Among the silicic samples, the enrichment and depletion of these elements are more pronounced. The only trachydacite ignimbrite studied in the La Reforma complex (LR1, $SiO_2 = 64.78\%$) has a smaller depletion in Nb, P, and Ti, similar to other rocks with similar silica content from another areas of La Pampa such as Algarrobo del Aguila. The enrichment in Th and U is also common for these rocks. The ignimbrites from Sierra de Lihue Calel and Sierra Chica, in the central part of La Pampa, have positive anomalies in Th and U (Sruoga and Llambías, 1992; Quenardelle and Llambías, 1997). Thus, we conclude that this anomalous behavior in Th and U is a common feature for the Choiyoi Group from La Pampa.

4. Discussion

The studied rocks form part of the Choiyoi Group from La Pampa province, which extends along a 230 km wide NW–SE belt. The general composition is similar to that of the Choiyoi Group elsewhere, such as in the San Rafael block and the Cordillera Frontal, where the Choiyoi is divided into an andesitic–dacitic lower section and a dacitic–rhyolitic upper section (Llambías et al., 1993).

The topography of the region was low when the volcanic activity of the Choiyoi Group began. Volcanic flows cover the Middle Proterozoic and Lower Paleozoic basement units, evidence that, in Permian times, these units were at the same crustal level. Middle Proterozoic tonalites and trondhjemites of Las Matras, Lower Paleozoic granodiorites and granites, Ordovician limestones of the San Jorge Formation, and metamorphic rocks of similar age were all exposed at the surface. The absence of rough relief during the Permian indicates that the Choiyoi Group evolved in a craton-like area adjacent to the orogenic front, which was located to the west in the San Rafael block (Fig. 1). Also, the fine-grained infilling of the Carapacha basin and its weak deformation (Melchor, 1999; Tomezzoli et al., 1999) agrees with the cratonic features of the Las Matras and Chadileuvú blocks.

The period before and coeval with the evolution of the Choiyoi Group was characterized by the development of a ductile NW shear belt (Tickyj et al., 1997) exposed in Paleozoic granites. K–Ar dating on the muscovite from the mylonites of Cerro Los Viejos yields an age of 254 ± 2 Ma (Tickyj, 1999), suggesting it was partially contemporaneous with the evolution of the Choiyoi Group in La Pampa. Both the NW major axis of the Carapacha basin (Melchor, 1999) and the NW rhyolite dike swarm of the Agua Escondida district (González Díaz, 1972) suggest an extensional regime with the minimum stress trending to the NE.

The relative tectonic stability in La Pampa at this time contrasts with the intense, compressive San Rafael orogenic phase in the Cordillera Frontal and San Rafael block. Therefore, unlike the geological evolution of these other regions, a postorogenic character cannot be attributed to the Choiyoi Group in La Pampa (Llambías and Sato, 1990, 1995; Llambías et al., 1993). In addition, the La Pampa units are marked by higher alkali content with respect to silica.

The shoshonitic rocks from Cerro Centinela and Lomas de Olguín plot in the field of the A-type granites (Fig. 11a) in the Zr versus 10,000 Ga/Al diagram (Whalen et al., 1987). The low CaO and high P_2O_5 and TiO_2 are also characteristic of A-type suites. The trachydacites and rhyolites plot close to the field of I- and S-type granites, are widely disperse without a definite trend, and maintain a high Ga/Al ratio, typical of peralkaline magmas (Collins et al., 1982).

In the Rb versus Y + Nb diagram (Fig. 11b), most of the rocks analyzed plot in the field of the magmatic arc granites, except for the Chos Malal granite and some rhyolite domes, whose compositions may have been modified by subsolidus reactions. The tectonic setting that arises from this diagram does not coincide with that of the Zr versus Ga/Al diagram, because the Rb versus Y + Nb diagram reflects characteristics of the source instead of the tectonic setting (Arculus, 1987; Twist and Harmer, 1987; Roberts and Clemens, 1993). Calc-alkaline tonalites and granodiorites are possible sources for peralkaline magmas (Anderson, 1983; Eby, 1990; Roberts and Clemens, 1993; Patiño Douce, 1997).

The high K_2O content agrees with a dehydration melting origin of the magma (Clemens et al., 1986), a process that requires high temperatures in the magma. The thermal minimum in the granite system moves toward albite with an increase in activity of the water. When melting takes place in subsaturated conditions, the resulting liquids are enriched in orthoclase with respect to albite (Becker et al., 1998).

The high temperature of the magma also can be inferred by the intense welding of the ignimbrites and their rheomorphic features (Fig. 4c and d), which are possible because the temperature of the magma during fragmentation was higher than the transition temperature of the glass (Freundt, 1998). Most of the ignimbrites described herein have rheomorphic features common to the Choiyoi Group of La Pampa (cf. Sruoga and Llambías, 1992; Quenardelle and Llambías, 1997).

Further evidence for high temperatures in the magma is the limited enrichment of LIL and HFS elements in the rhyolites, attributable to the high proportion of melting, which gave rise to the dilution of these incompatible elements in the melt. The high proportions of Th and U in almost all the samples, including those with the lowest silica content, may indicate a crustal source. A crustal source is also supported by the abundance of rhyolites with respect to less silicic compositions, in that the enormous volumes of primary magma required to produce the silicic differentiates are difficult to explain any other way.

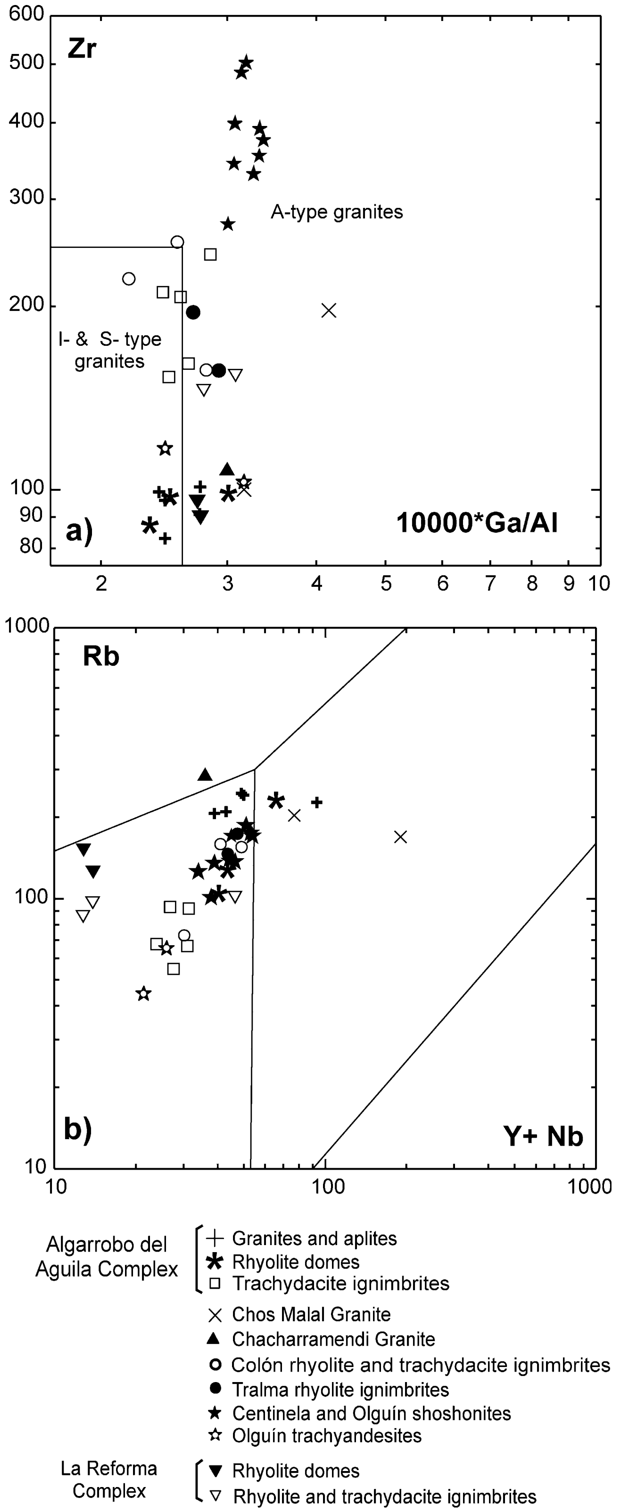

Fig. 11. Discrimination diagrams for the Choiyoi Group from northwestern La Pampa. (a) Zr versus 10,000 Ga/Al discrimination diagram for the typology of granites after Whalen et al. (1987). Most samples from the Choiyoi Group of La Pampa plot outside the field of the I- and S-type granites. Shoshonites from Cerro Centinela and Lomas de Olguín plot in the field of A-type granites. (b) Discrimination diagram for the tectonic setting of granites after Pearce et al. (1984). Most samples from the Choiyoi Group of La Pampa plot on the field of the magmatic arc.

The coeval extensional tectonic regime during the Late Permian and Early Triassic in La Pampa (Melchor, 1999; Tickyj, 1999) and a possible mafic underplate would have contributed to the high volumes of crustal melt. The origin of the mafic underplate may be related to the evolution of the Carboniferous–Lower Permian magmatic arc in the Cordillera Frontal. After subduction ceased in the Lower Permian (Kay et al., 1989; Llambías and Sato, 1990; Mpodozis and Kay, 1992), the energy of the magma decreased and was insufficient to drive the magma to the surface, which led to some of the mechanical discontinuities of the lithosphere (i.e. the Mohorovicic; Llambías, 2001).

5. Conclusions

The Choiyoi Group in La Pampa evolved in a cratonic environment adjacent to the active margin of the Gondwana continent, with major exposures to the west in the San Rafael block and the Cordillera Frontal, where the Choiyoi Group is clearly postorogenic. The Group consists of two suites: shoshonitic and trachydacitic-rhyolitic. They demonstrate a transitional signature between the subalkaline and alkaline series. In addition, they are enriched in alkali and TiO_2 and depleted in CaO in comparison with the postorogenic Choiyoi Group from the Cordillera Frontal. The shoshonitic suite is unusually enriched in P_2O_5 and Sr and depleted in Nb. Both suites also are enriched in Th and U, common to the Choiyoi Group in La Pampa. The ignimbrites of both suites have rheomorphic textures, consistent with high temperatures and low particle viscosity during emplacement (Freundt, 1998) and typical of intraplate volcanism.

We postulate a crustal origin for the magma with calc-alkaline source rocks. The extensional tectonic regime that prevailed during the evolution of the Choiyoi Group favored melting processes.

Although the Choiyoi Group in La Pampa evolved over different basements, including the exotic Cuyania terrane and the active margin of the Gondwana continent during the Lower Paleozoic (Pampia terrane), there are no differences in lithology and chemical signatures.

Acknowledgements

We are grateful to Ricardo Melchor and Hugo Tickyj for helpful discussion about the geology of the study area. The Argentinian government provided financial support through the Agencia Nacional de Promoción Científica y Tecnológica, PICT 0743, and CONICET, PIP 4329/96 and PEI 148/97. Constructive comments by Víctor Ramos and reviews by Susan Mahlburg Kay and Constatino Mpodozis improved and helped significantly clarify the contents.

References

Anderson, J.L., 1983. Proterozoic anorogenic granite plutonism of North America. Geological Society of America Memoir 161, 133–154.

Arculus, R.J., 1987. The significance of source versus process in the tectonic control of the magma genesis. Journal of Volcanology and Geothermal Research 32, 1–12.

Astini, R., Benedetto, J., Vaccari, N., 1995. The early Paleozoic evolution of the Argentine Precordillera as a Laurentian rifted, drifted and collided terrane, a geodynamic model. Geological Society of America Bulletin 107, 253–273.

Becker, A., Holtz, F., Johannes, W., 1998. Liquidus temperatures and phase compositions in the system Qz–Ab–Or at 5 kbar and very low water activities. Contributions to Mineralogy and Petrology 130, 213–224.

Caminos, R., 1979. Cordillera Frontal. In: Turner, J.C.M., (Ed.), Segundo Simposio de Geología Regional de Argentina, Academia Nacional de Ciencias, Córdoba, pp. 398–453.

Caminos, R., Azcuy, C., 1991. Fases diastróficas neopaleozoicas. In: Archangelsky, S., (Ed.), El Sistema Pérmico en la República Argentina y en la República Oriental del Uruguay, XII Congreso Internacional de la Estratigrafía y Geología del Carbonífero y del Pérmico, Academia Nacional de Ciencias, Córdoba, pp. 255–265.

Clemens, J.D., Holloway, J.R., White, A.J.R., 1986. Origin of A-type granites: experimental constraints. American Mineralogist 71, 317–324.

Collins, W.J., Beams, S.D., White, A.J.R., Chappel, B.W., 1982. Nature and origin of A-type granites with particular reference to southeastern Australia. Contributions to Mineralogy and Petrology 80, 189–200.

Dalla Salda, L.H., Cingolani, C., Varela, R., 1992. Early Paleozoic orogenic belt of the Andes in southwestern South America: result of Laurentia-Gondwana collision? Geology 20, 617–620.

Eby, G.N., 1990. The A-type granitoids: a review of their occurrence and chemical characterisitics and speculations on their petrogenesis. Lithos 26, 115–134.

Freundt, A., 1998. The formation of high-grade ignimbrites, I: experiments on high- and low-concentration transport systems containing sticky particles. Bulletin of Volcanology 59, 414–435.

Gill, J., 1981. Orogenic andesites and plate tectonics, Springer, Berlin, p. 390.

González Díaz, E.F., 1972. Descripción geológica de la Hoja 30e, Agua Escondida, provincias de Mendoza y la Pampa. Servicio Nacional Minero Geológico Boletín 135, 1–78.

Irvine, T.N., Baragar, W.R.A., 1971. A guide to the chemical classification of the common rocks. Canadian Journal Earth Sciences 8, 523–548.

Kay, S.M., Ramos, V.A., Mpodozis, C., Sruoga, P., 1989. Late Paleozoic to Jurassic silicic magmatism at the Gondwanaland margin: analogy to the Middle Proterozoic in North America? Geology 17, 324–328.

Le Maitre, R.W., 1976. Some problems of the projection of chemical data in mineralogical classifications. Contributions to Mineralogy and Petrology 56, 181–189.

Le Maitre, R.W., Streckeisen, A., Zanettin, B., Le Bas, M.J., Bonin, B., Bateman, P., Bellieni, G., Dudek, A., Efremova, S., Keller, J., Lameyre, J., Sabine, P.A., Schmid, R., Sørensen, H., Woolley, A.R. (Eds.), 2002. Igneous Rocks: A Classification and Glossary of Terms. Recommendations of the International Union of Geological Sciences Subcommission on the Systematics of Igneous Rocks. Cambridge University Press, p. 236.

Linares, E., Llambías, E.J., Latorre, C.O., 1980. Geología de la provincia de La Pampa, República Argentina y geocronología de sus rocas metamórficas y eruptivas. Revista de la Asociación Geológica Argentina 35, 87–146.

Llambías, E.J., 2001. Complejos magmáticos triásicos al norte de los 40°S. In: Artabe, A.E., Morel, E.M., Zamuner, A.B. (Eds.), El Sistema Triásico en la Argentina, Fundación Museo de La Plata Francisco Pascasio Moreno, La Plata, pp. 55–68.

Llambías, E.J., Leveratto, M.A., 1975. El plateau riolítico de la provincia de La Pampa, República Argentina. 2 Congreso Iberoamericano de Geología Económica, Buenos Aires, Actas 1, 99–114.

Llambías, E.J., Sato, A.M., 1990. El batolito de Colangüil (29–31°S) Cordillera Frontal de Argentina: estructura y marco tectónico. Revista Geológica de Chile 17, 99–108.

Llambías, E.J., Sato, A.M., 1995. Tectónica y magmatismo en el límite Pérmico-Triásico de la Cordillera Frontal. Acta II Segunda Reunión del Triásico del Cono Sur, Bahía Blanca, 22–26.

Llambías, E.J., Sato, A.M., Castro, C.E., 1990. Relaciones entre el Grupo Choiyoi y el batolito de Colangüil. XI Congreso Geológico Argentino, San Juan, Actas 1, 99–108.

Llambías, E.J., Kleiman, L.E., Salvarredi, J.A., 1993. El Magmatismo Gondwánico. In: Ramos, V.A., (Ed.), Geología y Recursos Naturales de Mendoza, Relatorio, XII Congreso Geológico Argentino y II Congreso de Exploración de Hidrocarburos (Mendoza), pp. 53–64.

Llambías, E.J., Melchor, R.N., Tickyj, H., Sato, A.M., 1996. Geología del Bloque del Chadileuvú. XIII Congreso Geológico Argentino y III Congreso de Exploración de Hidrocarburos, Actas V, 417–425.

Melchor, R.N., 1999. Redefinición estratigráfica de la Formación Carapacha (Pérmico), Provincia de La Pampa. Revista de la Asociación Geológica Argentina 54 (2), 99–108.

Melchor, R.N., Sato, A.M., Llambías, E.J., Tickyj, H., 1999. Documentación de la extensión meridional del terreno Cuyania/Precordillera en la provincia de La Pampa. XIV Congreso Geológico Argentino, Actas I, 156–159.

Morrison, G.W., 1980. Characteristics and tectonic setting of the shoshonite rock association. Lithos 13, 97–108.

Mpodozis, C., Kay, S.M., 1992. Late Paleozoic to Triassic evolution of the Gondwana margin: Evidence from Chilean Frontal Cordilleran batholiths (28°S to 31°S). Geological Society of America Bulletin 104, 999–1014.

Nasi, C., Mpodozis, C., Cornejo, P., Moscoso, R., Maksaev, V., 1985. El batolito Elqui-Limarí (Paleozoico superior-Triásico): características petrográficas, geoquímicas y significado tectónico. Revista Geológica de Chile 25/26, 77–111.

Patiño Douce, A.E., 1997. Generation of metaluminous A-type granites by low-pressure melting of calc-alkaline granitoids. Geology 25, 743–746.

Pearce, J.A., Harris, N.B.W., Tindle, A.G., 1984. Trace element discrimination diagrams for the tectonic interpretation of granitic rocks. Journal of Petrology 25, 956–983.

Peccerillo, A., Taylor, S.R., 1976. Geochemistry of Eocene calc-alkaline volcanic rocks from the Kastamonu area, northern Turkey. Contributions to Mineralogy and Petrology 58, 63–81.

Pitcher, W.S., Atherton, M.P., Cobbing, E.J., Beckinsale, R.D., 1985. Magmatism at a Plate Edge, The Peruvian Andes, Blackie, Londres, p. 328.

Quenardelle, S.M., Llambías, E.J., 1997. Las riolitas de Sierra Chica (37°48′S, 65°26′O): un centro eruptivo gondwánico en el bloque del Chadileuvú, provincia de La Pampa, Argentina. Revista de la Asociación Geológica Argentina 52 (4), 549–558.

Ramos, V.A., 1999. Evolución Tectónia de la Argentina. In: Caminos, R., (Ed.), Geología Argentina, Anales 29 (24), Instituto de Geología y Recursos Minerales, Buenos Aires, pp. 715–784.

Ramos, V.A., Dallmeyer, R.D., Vujovich, G., 1998. Time constraints on the Early Paleozoic docking of the Precordillera, central Argentina. In: Pankhurst, R.J., Rapela, C.W. (Eds.), The Proto-Andean Margin of Gondwana, Geological Society London, Special Publication 142, pp. 143–158.

Rapalini, A.E., Vilas, J.F., 1991. Tectonic rotations in the Late Paleozoic continental margin of southern South America determined and dated by paleomagnetism. Geophysical Journal International 107, 333–351.

Roberts, M.P., Clemens, J.D., 1993. Origin of high-potassium, calc-alkaline, I-type granitoids. Geology 21, 825–828.

Sato, A.M., Llambías, E.J., 1993. El Grupo Choiyoi, provincia de San Juan: equivalente efusivo del Batolito de Colangüil. XII Congreso Geológico

Argentino y II Congreso de Exploración de Hidrocarburos (Mendoza), Actas IV, 156–165.

Sato, A.M., Tickyj, H., Llambías, E.J., 1996. Geología de los afloramientos graníticos del sur de la provincia de La Pampa. XIII Congreso Geológico Argentino y III Congreso de Exploración de Hidrocarburos (Buenos Aires), Actas V, 429–439.

Sato, A.M., Tickyj, H., Llambías, E.J., Sato, K., 1999. Rb–Sr, Sm–Nd and K–Ar age constraints of the Grenvillian Las Matras pluton, Central Argentina. Actas II South American Symposium on Isotope Geology. Servicio Geológico Minero Argentino, Anales 34, 122–126.

Sato, A.M., Tickyj, H., Llambías, E.J., Sato, K., 2000. The Las Matras tonalitic-trondhjemitic pluton, Central Argentina: Grenvillian age constraints, geochemical characteristics, and regional implications. Journal of South American Earth Sciences 13, 587–610.

SEGEMAR, 1998. Levantamiento geofísico aéreo. Magnetometría y espectrometría de rayos gamma, área San Rafael (Mendoza y La Pampa). Proyecto Pasma, Hoja Santa Isabel 3766I, Servicio Geológico Minero Argentino, Buenos Aires.

Sruoga, P., Llambías, E.J., 1992. Permo-Triassic leucorhyolitic ignimbrites at Sierra de Lihue Calel, La Pampa province, Argentina. Journal of South American Earth Sciences 5, 141–152.

Taylor, S.R., McLennan, S.M., 1985. The Continental Crust: Its composition and Evolution, Blackwell, Oxford, p. 312.

Tickyj, H., 1999. Estructura y petrología del basamento cristalino en la región centro-sur de la provincia de La Pampa, Argentina. Tesis de Doctor, Facultad de Ciencias Naturales y Museo, UNLP, La Plata, p. 229.

Tickyj, H., Dimieri, L.V., Llambías, E.J., Sato, A.M., 1997. Cerro Los Viejos (38° 28′S–64°26′O): cizallamiento dúctil en el sudeste de La Pampa. Revista de la Asociación Geológica Argentina 52 (3), 311–321.

Tickyj, H., Llambías, E.J., Sato, A.M., 1999. El basamento cristalino de la región suroriental de la provincia de La Pampa: extensión austral del orógeno Famatiniano de Sierras Pampeanas. XIV Congreso Geológico Argentino (Salta), Actas I, 160–163.

Tomezzoli, R.N., MacDonald, W.D., Melchor, R.N., 1999. Análisis de la anisotropía de susceptibilidad magnética de la Cuenca Carapacha (Pérmico), centro-sur de La Pampa, Argentina. XIV Congreso Geológico Argentino (Salta), Actas I, 164–167.

Twist, D., Harmer, R.E.J., 1987. Geochemistry of contrasting siliceous magmatic suites in the Bushveld complex: Genetic aspects and the implication for the tectonic discrimination diagrams. Journal of Volcanology and Geothermal Research 32, 83–98.

Vujovich, G.I., Kay, S.M.A., 1998. A Laurentian? Grenville-age oceanic arc/back-arc terrane in the Sierra de Pie de Palo, Western Sierras Pampeanas, Argentina. In: Pankhurst, R., Rapela, C.W. (Eds.), The Proto-Andean Margin of Gondwana, Geological Society of London, Special Publication 142, pp. 159–179.

Whalen, J.B., Currie, K.L., Chappel, B.W., 1987. A-type granites: geochemical characteristics, discrimination and petrogenesis. Contributions to Mineralogy and Petrology 95, 407–419.